



When plane light waves pass through a small aperture in an opaque barrier, the aperture acts as if it were a point source of light, with waves entering the shadow region behind the barrier. This phenomenon, known as diffraction, can be described only with a wave model for light, as discussed in Section 35.3. In this chapter, we investigate the features of the *diffraction pattern* that occurs when the light from the aperture is allowed to fall upon a screen.

In Chapter 34, we learned that electromagnetic waves are transverse. That is, the electric and magnetic field vectors associated with electromagnetic waves are perpendicular to the direction of wave propagation. In this chapter, we show that under certain conditions these transverse waves with electric field vectors in all possible transverse directions can be *polarized* in various ways. This means that only certain directions of the electric field vectors are present in the polarized wave.

38.1 Introduction to Diffraction Patterns

In Section 35.3 we discussed the fact that light of wavelength comparable to or larger than the width of a slit spreads out in all forward directions upon passing through the slit. We call this phenomenon *diffraction*. This behavior indicates that light, once it has passed through a narrow slit, spreads beyond the narrow path defined by the slit into regions that would be in shadow if light traveled in straight lines. Other waves, such as sound waves and water waves, also have this property of spreading when passing through apertures or by sharp edges.

We might expect that the light passing through a small opening would simply result in a broad region of light on a screen, due to the spreading of the light as it passes through the opening. We find something more interesting, however. A **diffraction pattern** consisting of light and dark areas is observed, somewhat similar to the interference patterns discussed earlier. For example, when a narrow slit is placed between a distant light source (or a laser beam) and a screen, the light produces a diffraction pattern like that in Figure 38.1. The pattern consists of a broad, intense central band (called the **central maximum**), flanked by a series of narrower, less intense additional bands (called **side maxima** or **secondary maxima**) and a series of intervening dark bands (or **minima**). Figure 38.2 shows a diffraction pattern associated with light passing by the edge of an object. Again we see bright and dark fringes, which is reminiscent of an interference pattern.

Figure 38.3 shows a diffraction pattern associated with the shadow of a penny. A bright spot occurs at the center, and circular fringes extend outward from the shadow's edge. We can explain the central bright spot only by using the wave theory of light, which predicts constructive interference at this point. From the viewpoint of geometric optics (in which light is viewed as rays traveling in straight lines), we expect the center of the shadow to be dark because that part of the viewing screen is completely shielded by the penny.

It is interesting to point out an historical incident that occurred shortly before the central bright spot was first observed. One of the supporters of geometric optics,

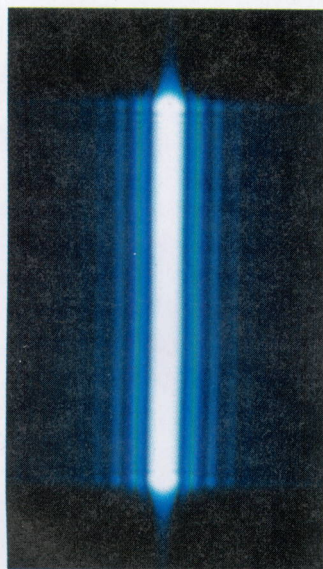


Figure 38.1 The diffraction pattern that appears on a screen when light passes through a narrow vertical slit. The pattern consists of a broad central fringe and a series of less intense and narrower side fringes.

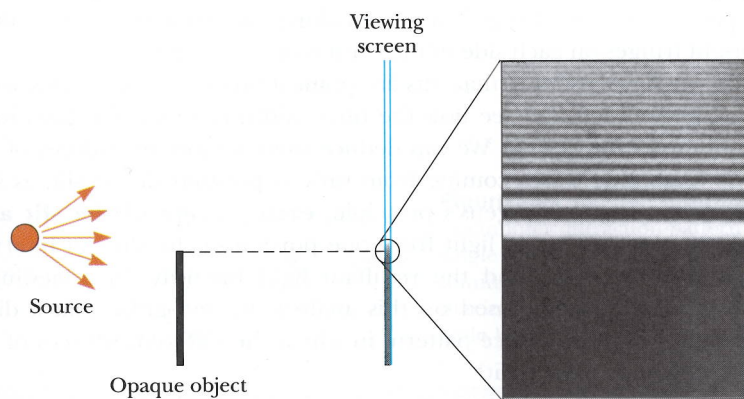


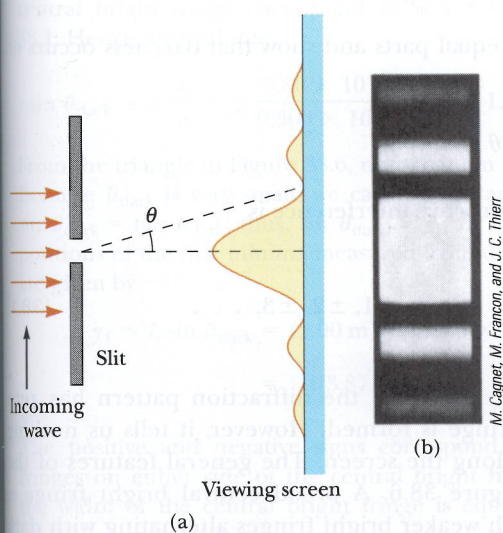
Figure 38.2 Light from a small source passes by the edge of an opaque object and continues on to a screen. A diffraction pattern consisting of bright and dark fringes appears on the screen in the region above the edge of the object.

Simeon Poisson, argued that if Augustin Fresnel's wave theory of light were valid, then a central bright spot should be observed in the shadow of a circular object illuminated by a point source of light. To Poisson's astonishment, the spot was observed by Dominique Arago shortly thereafter. Thus, Poisson's prediction reinforced the wave theory rather than disproving it.

38.2 Diffraction Patterns from Narrow Slits

Let us consider a common situation, that of light passing through a narrow opening modeled as a slit, and projected onto a screen. To simplify our analysis, we assume that the observing screen is far from the slit, so that the rays reaching the screen are approximately parallel. This can also be achieved experimentally by using a converging lens to focus the parallel rays on a nearby screen. In this model, the pattern on the screen is called a **Fraunhofer diffraction pattern**.¹

Figure 38.4a shows light entering a single slit from the left and diffracting as it propagates toward a screen. Figure 38.4b is a photograph of a single-slit Fraunhofer diffraction pattern.



Active Figure 38.4 (a) Fraunhofer diffraction pattern of a single slit. The pattern consists of a central bright fringe flanked by much weaker maxima alternating with dark fringes. (Drawing not to scale.) (b) Photograph of a single-slit Fraunhofer diffraction pattern.

¹ If the screen is brought close to the slit (and no lens is used), the pattern is a *Fresnel* diffraction pattern. The Fresnel pattern is more difficult to analyze, so we shall restrict our discussion to Fraunhofer diffraction.

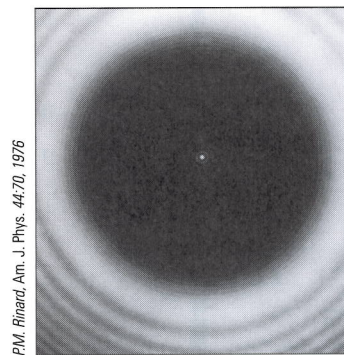



Figure 38.3 Diffraction pattern created by the illumination of a penny, with the penny positioned midway between screen and light source. Note the bright spot at the center.

▲ PITFALL PREVENTION

38.1 Diffraction vs. Diffraction Pattern

Diffraction refers to the general behavior of waves spreading out as they pass through a slit. We used diffraction in explaining the existence of an interference pattern in Chapter 37. A *diffraction pattern* is actually a misnomer but is deeply entrenched in the language of physics. The diffraction pattern seen on a screen when a single slit is illuminated is really another interference pattern. The interference is between parts of the incident light illuminating different regions of the slit.

 **At the Active Figures link at <http://www.pse6.com>, you can adjust the slit width and the wavelength of the light to see the effect on the diffraction pattern.**

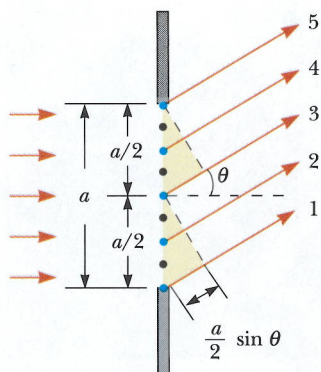


Figure 38.5 Paths of light rays that encounter a narrow slit of width a and diffract toward a screen in the direction described by angle θ . Each portion of the slit acts as a point source of light waves. The path difference between rays 1 and 3, rays 2 and 4, or rays 3 and 5 is $(a/2) \sin \theta$. (Drawing not to scale.)

▲ PITFALL PREVENTION

38.2 Similar Equation Warning!

Equation 38.1 has exactly the same form as Equation 37.2, with d , the slit separation, used in Equation 37.2 and a , the slit width, in Equation 38.1. However, Equation 37.2 describes the *bright* regions in a two-slit interference pattern while Equation 38.1 describes the *dark* regions in a single-slit diffraction pattern. Furthermore, $m = 0$ does not represent a dark fringe in the diffraction pattern.

Condition for destructive interference for a single slit

diffraction pattern. A bright fringe is observed along the axis at $\theta = 0$, with alternating dark and bright fringes on each side of the central bright fringe.

Until now, we have assumed that slits are point sources of light. In this section, we abandon that assumption and see how the finite width of slits is the basis for understanding Fraunhofer diffraction. We can deduce some important features of this phenomenon by examining waves coming from various portions of the slit, as shown in Figure 38.5. According to Huygens's principle, **each portion of the slit acts as a source of light waves**. Hence, light from one portion of the slit can interfere with light from another portion, and the resultant light intensity on a viewing screen depends on the direction θ . Based on this analysis, we recognize that a diffraction pattern is actually an interference pattern, in which the different sources of light are different portions of the single slit!

To analyze the diffraction pattern, it is convenient to divide the slit into two halves, as shown in Figure 38.5. Keeping in mind that all the waves are in phase as they leave the slit, consider rays 1 and 3. As these two rays travel toward a viewing screen far to the right of the figure, ray 1 travels farther than ray 3 by an amount equal to the path difference $(a/2) \sin \theta$, where a is the width of the slit. Similarly, the path difference between rays 2 and 4 is also $(a/2) \sin \theta$, as is that between rays 3 and 5. If this path difference is exactly half a wavelength (corresponding to a phase difference of 180°), then the two waves cancel each other and destructive interference results. If this is true for two such rays, then it is true for any two rays that originate at points separated by half the slit width because the phase difference between two such points is 180° . Therefore, waves from the upper half of the slit interfere destructively with waves from the lower half when

$$\frac{a}{2} \sin \theta = \pm \frac{\lambda}{2}$$

or when

$$\sin \theta = \pm \frac{\lambda}{a}$$

If we divide the slit into four equal parts and use similar reasoning, we find that the viewing screen is also dark when

$$\sin \theta = \pm \frac{2\lambda}{a}$$

Likewise, we can divide the slit into six equal parts and show that darkness occurs on the screen when

$$\sin \theta = \pm \frac{3\lambda}{a}$$

Therefore, the general condition for destructive interference is

$$\sin \theta_{\text{dark}} = m \frac{\lambda}{a} \quad m = \pm 1, \pm 2, \pm 3, \dots \quad (38.1)$$

This equation gives the values of θ_{dark} for which the diffraction pattern has zero light intensity—that is, when a dark fringe is formed. However, it tells us nothing about the variation in light intensity along the screen. The general features of the intensity distribution are shown in Figure 38.6. A broad central bright fringe is observed; this fringe is flanked by much weaker bright fringes alternating with dark fringes. The various dark fringes occur at the values of θ_{dark} that satisfy Equation 38.1. Each bright-fringe peak lies approximately halfway between its bordering dark-fringe minima. Note that the central bright maximum is twice as wide as the secondary maxima.

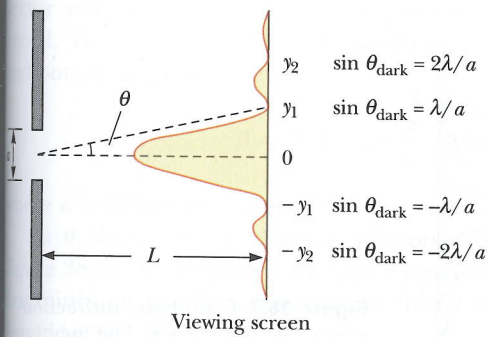


Figure 38.6 Intensity distribution for a Fraunhofer diffraction pattern from a single slit of width a . The positions of two minima on each side of the central maximum are labeled. (Drawing not to scale.)

Quick Quiz 38.1 Suppose the slit width in Figure 38.6 is made half as wide. The central bright fringe (a) becomes wider (b) remains the same (c) becomes narrower.

Quick Quiz 38.2 If a classroom door is open slightly, you can hear sounds coming from the hallway. Yet you cannot see what is happening in the hallway. Why is there this difference? (a) Light waves do not diffract through the single slit of the open doorway. (b) Sound waves can pass through the walls, but light waves cannot. (c) The open door is a small slit for sound waves, but a large slit for light waves. (d) The open door is a large slit for sound waves, but a small slit for light waves.

Example 38.1 Where Are the Dark Fringes?

Interactive

Light of wavelength 580 nm is incident on a slit having a width of 0.300 mm. The viewing screen is 2.00 m from the slit. Find the positions of the first dark fringes and the width of the central bright fringe.

Solution The problem statement cues us to conceptualize a single-slit diffraction pattern similar to that in Figure 38.6. We categorize this as a straightforward application of our discussion of single-slit diffraction patterns. To analyze the problem, note that the two dark fringes that flank the central bright fringe correspond to $m = \pm 1$ in Equation 38.1. Hence, we find that

$$\sin \theta_{\text{dark}} = \pm \frac{\lambda}{a} = \pm \frac{5.80 \times 10^{-7} \text{ m}}{0.300 \times 10^{-3} \text{ m}} = \pm 1.933 \times 10^{-3}$$

From the triangle in Figure 38.6, note that $\tan \theta_{\text{dark}} = y_1/L$. Because θ_{dark} is very small, we can use the approximation $\sin \theta_{\text{dark}} \approx \tan \theta_{\text{dark}}$; thus, $\sin \theta_{\text{dark}} \approx y_1/L$. Therefore, the positions of the first minima measured from the central axis are given by

$$\begin{aligned} y_1 &\approx L \sin \theta_{\text{dark}} = (2.00 \text{ m})(\pm 1.933 \times 10^{-3}) \\ &= \pm 3.87 \times 10^{-3} \text{ m} \end{aligned}$$

The positive and negative signs correspond to the dark fringes on either side of the central bright fringe. Hence, the width of the central bright fringe is equal to $2|y_1| = 7.74 \times 10^{-3} \text{ m} = 7.74 \text{ mm}$. To finalize this problem,

note that this value is much greater than the width of the slit. We finalize further by exploring what happens if we change the slit width.

What If? What if the slit width is increased by an order of magnitude to 3.00 mm? What happens to the diffraction pattern?

Answer Based on Equation 38.1, we expect that the angles at which the dark bands appear will decrease as a increases. Thus, the diffraction pattern narrows. For $a = 3.00 \text{ mm}$, the sines of the angles θ_{dark} for the $m = \pm 1$ dark fringes are

$$\sin \theta_{\text{dark}} = \pm \frac{\lambda}{a} = \pm \frac{5.80 \times 10^{-7} \text{ m}}{3.00 \times 10^{-3} \text{ m}} = \pm 1.933 \times 10^{-4}$$

The positions of the first minima measured from the central axis are given by

$$\begin{aligned} y_1 &\approx L \sin \theta_{\text{dark}} = (2.00 \text{ m})(\pm 1.933 \times 10^{-4}) \\ &= \pm 3.87 \times 10^{-4} \text{ m} \end{aligned}$$

and the width of the central bright fringe is equal to $2|y_1| = 7.74 \times 10^{-4} \text{ m} = 0.774 \text{ mm}$. Notice that this is *smaller* than the width of the slit.

In general, for large values of a , the various maxima and minima are so closely spaced that only a large central bright area resembling the geometric image of the slit is observed. This is very important in the performance of optical instruments such as telescopes.

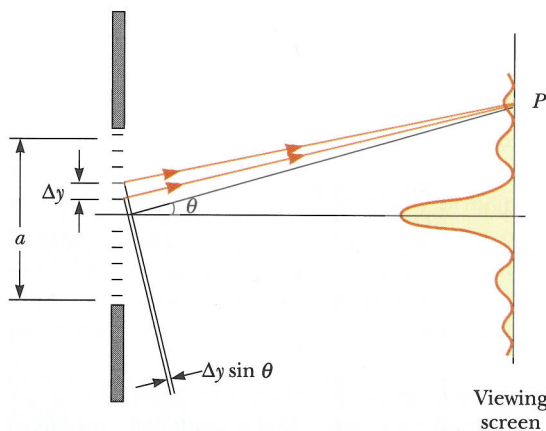


Figure 38.7 Fraunhofer diffraction pattern for a single slit. The light intensity at a distant screen is the resultant of all the incremental electric field magnitudes from zones of width Δy .

Intensity of Single-Slit Diffraction Patterns

We can use phasors to determine the light intensity distribution for a single-slit diffraction pattern. Imagine a slit divided into a large number of small zones, each of width Δy as shown in Figure 38.7. Each zone acts as a source of coherent radiation, and each contributes an incremental electric field of magnitude ΔE at some point on the screen. We obtain the total electric field magnitude E at a point on the screen by summing the contributions from all the zones. The light intensity at this point is proportional to the square of the magnitude of the electric field (Section 37.3).

The incremental electric field magnitudes between adjacent zones are out of phase with one another by an amount $\Delta\beta$, where the phase difference $\Delta\beta$ is related to the path difference $\Delta y \sin \theta$ between adjacent zones by an expression given by an argument similar to that leading to Equation 37.8:

$$\Delta\beta = \frac{2\pi}{\lambda} \Delta y \sin \theta \quad (38.2)$$

To find the magnitude of the total electric field on the screen at any angle θ , we sum the incremental magnitudes ΔE due to each zone. For small values of θ , we can assume that all the ΔE values are the same. It is convenient to use phasor diagrams for various angles, as in Figure 38.8. When $\theta = 0$, all phasors are aligned as in Figure 38.8a because all the waves from the various zones are in phase. In this case, the total electric field at the center of the screen is $E_0 = N\Delta E$, where N is the number of zones. The resultant magnitude E_R at some small angle θ is shown in Figure 38.8b, where each phasor differs in phase from an adjacent one by an amount $\Delta\beta$. In this case, E_R is the

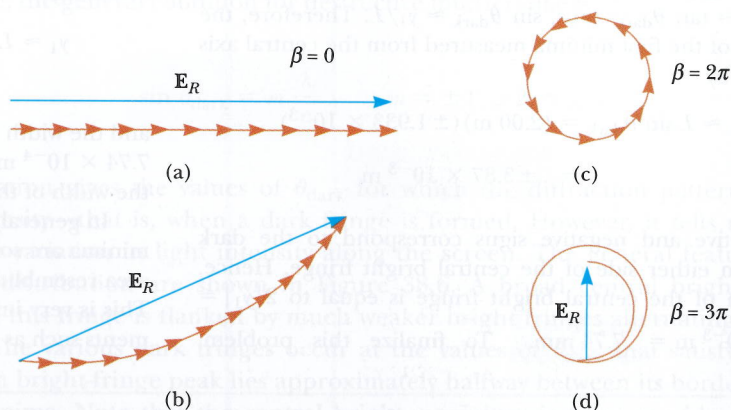


Figure 38.8 Phasor diagrams for obtaining the various maxima and minima of a single-slit diffraction pattern.

vector sum of the incremental magnitudes and hence is given by the length of the chord. Therefore, $E_R < E_0$. The total phase difference β between waves from the top and bottom portions of the slit is

$$\beta = N \Delta\beta = \frac{2\pi}{\lambda} N \Delta y \sin\theta = \frac{2\pi}{\lambda} a \sin\theta \quad (38.3)$$

where $a = N \Delta y$ is the width of the slit.

As θ increases, the chain of phasors eventually forms the closed path shown in Figure 38.8c. At this point, the vector sum is zero, and so $E_R = 0$, corresponding to the first minimum on the screen. Noting that $\beta = N \Delta\beta = 2\pi$ in this situation, we see from Equation 38.3 that

$$2\pi = \frac{2\pi}{\lambda} a \sin\theta_{\text{dark}}$$

$$\sin\theta_{\text{dark}} = \frac{\lambda}{a}$$

That is, the first minimum in the diffraction pattern occurs where $\sin\theta_{\text{dark}} = \lambda/a$; this is in agreement with Equation 38.1.

At larger values of θ , the spiral chain of phasors tightens. For example, Figure 38.8d represents the situation corresponding to the second maximum, which occurs when $\beta = 360^\circ + 180^\circ = 540^\circ$ (3π rad). The second minimum (two complete circles, not shown) corresponds to $\beta = 720^\circ$ (4π rad), which satisfies the condition $\sin\theta_{\text{dark}} = 2\lambda/a$.

We can obtain the total electric-field magnitude E_R and light intensity I at any point on the screen in Figure 38.7 by considering the limiting case in which Δy becomes infinitesimal (dy) and N approaches ∞ . In this limit, the phasor chains in Figure 38.8 become the curve of Figure 38.9. The arc length of the curve is E_0 because it is the sum of the magnitudes of the phasors (which is the total electric field magnitude at the center of the screen). From this figure, we see that at some angle θ , the resultant electric field magnitude E_R on the screen is equal to the chord length. From the triangle containing the angle $\beta/2$, we see that

$$\sin \frac{\beta}{2} = \frac{E_R/2}{R}$$

where R is the radius of curvature. But the arc length E_0 is equal to the product $R\beta$, where β is measured in radians. Combining this information with the previous expression gives

$$E_R = 2R \sin \frac{\beta}{2} = 2 \left(\frac{E_0}{\beta} \right) \sin \frac{\beta}{2} = E_0 \left[\frac{\sin(\beta/2)}{\beta/2} \right]$$

Because the resultant light intensity I at a point on the screen is proportional to the square of the magnitude E_R , we find that

$$I = I_{\text{max}} \left[\frac{\sin(\beta/2)}{\beta/2} \right]^2 \quad (38.4)$$

where I_{max} is the intensity at $\theta = 0$ (the central maximum). Substituting the expression for β (Eq. 38.3) into Equation 38.4, we have

$$I = I_{\text{max}} \left[\frac{\sin(\pi a \sin\theta/\lambda)}{\pi a \sin\theta/\lambda} \right]^2 \quad (38.5)$$

From this result, we see that *minima* occur when

$$\frac{\pi a \sin\theta_{\text{dark}}}{\lambda} = m\pi$$

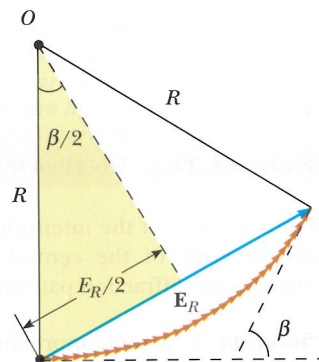
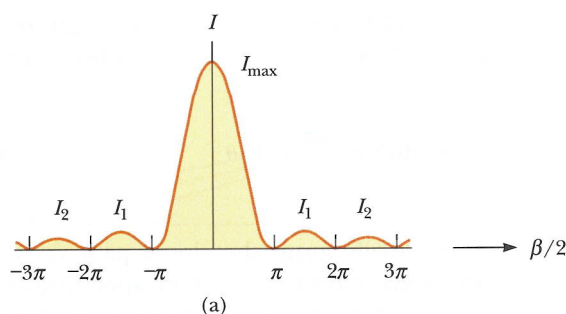
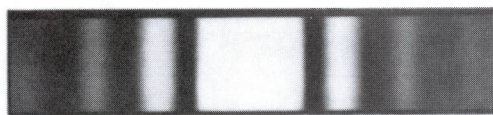


Figure 38.9 Phasor diagram for a large number of coherent sources. All the ends of the phasors lie on the circular arc of radius R . The resultant electric field magnitude E_R equals the length of the chord.

Intensity of a single-slit Fraunhofer diffraction pattern



M. Cagnet, M. Francon,
and J. C. Thier



(b)

Figure 38.10 (a) A plot of light intensity I versus $\beta/2$ for the single-slit Fraunhofer diffraction pattern. (b) Photograph of a single-slit Fraunhofer diffraction pattern.

or

Condition for intensity minima for a single slit

$$\sin \theta_{\text{dark}} = m \frac{\lambda}{a} \quad m = \pm 1, \pm 2, \pm 3, \dots$$

in agreement with Equation 38.1.

Figure 38.10a represents a plot of Equation 38.4, and Figure 38.10b is a photograph of a single-slit Fraunhofer diffraction pattern. Note that most of the light intensity is concentrated in the central bright fringe.

Example 38.2 Relative Intensities of the Maxima

Find the ratio of the intensities of the secondary maxima to the intensity of the central maximum for the single-slit Fraunhofer diffraction pattern.

Solution To a good approximation, the secondary maxima lie midway between the zero points. From Figure 38.10a, we see that this corresponds to $\beta/2$ values of $3\pi/2$, $5\pi/2$, $7\pi/2$, \dots . Substituting these values into Equation 38.4 gives for the first two ratios

$$\frac{I_1}{I_{\text{max}}} = \left[\frac{\sin(3\pi/2)}{(3\pi/2)} \right]^2 = \frac{1}{9\pi^2/4} = 0.045$$

$$\frac{I_2}{I_{\text{max}}} = \left[\frac{\sin(5\pi/2)}{5\pi/2} \right]^2 = \frac{1}{25\pi^2/4} = 0.016$$

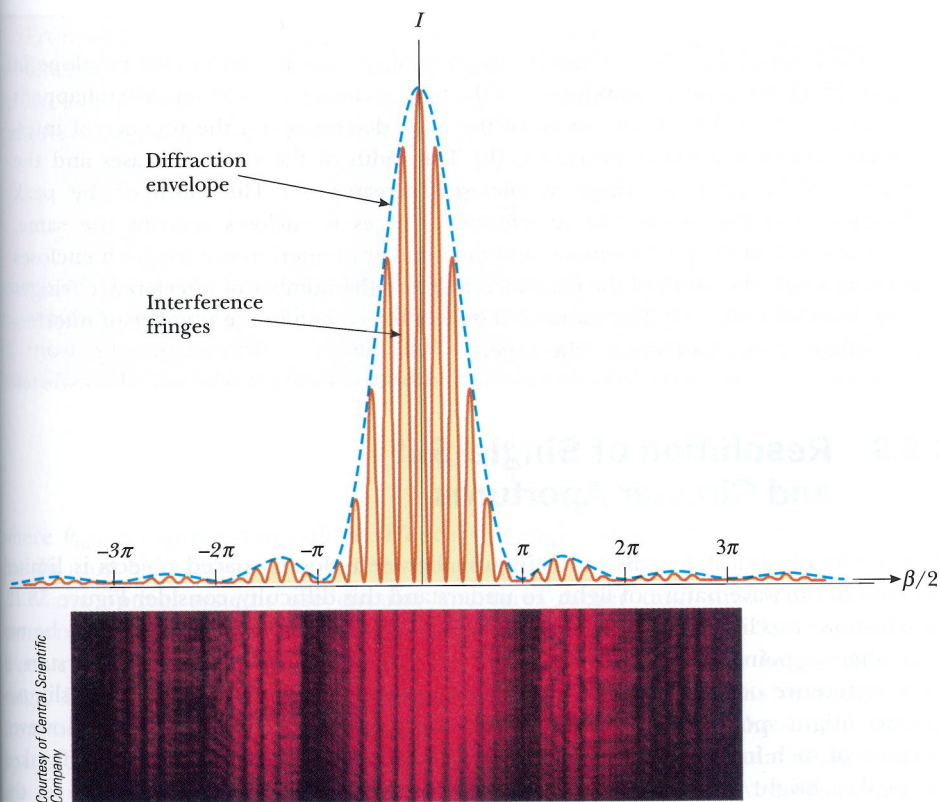
That is, the first secondary maxima (the ones adjacent to the central maximum) have an intensity of 4.5% that of the central maximum, and the next secondary maxima have an intensity of 1.6% that of the central maximum.

Intensity of Two-Slit Diffraction Patterns


When more than one slit is present, we must consider not only diffraction patterns due to the individual slits but also the interference patterns due to the waves coming from different slits. Notice the curved dashed lines in Figure 37.14, which indicate a decrease in intensity of the interference maxima as θ increases. This decrease is due to a diffraction pattern. To determine the effects of both two-slit interference and a single-slit diffraction pattern from each slit, we combine Equations 37.12 and 38.5:

$$I = I_{\text{max}} \cos^2 \left(\frac{\pi d \sin \theta}{\lambda} \right) \left[\frac{\sin(\pi a \sin \theta / \lambda)}{\pi a \sin \theta / \lambda} \right]^2 \quad (38.6)$$

Although this expression looks complicated, it merely represents the single-slit diffraction pattern (the factor in square brackets) acting as an “envelope” for a two-slit



Active Figure 38.11 The combined effects of two-slit and single-slit interference. This is the pattern produced when 650-nm light waves pass through two 3.0- μm slits that are 18 μm apart. Notice how the diffraction pattern acts as an “envelope” and controls the intensity of the regularly spaced interference maxima.

 **At the Active Figures link at <http://www.pse6.com>, you can adjust the slit width, slit separation, and the wavelength of the light to see the effect on the interference pattern.**

interference pattern (the cosine-squared factor), as shown in Figure 38.11. The broken blue curve in Figure 38.11 represents the factor in square brackets in Equation 38.6. The cosine-squared factor by itself would give a series of peaks all with the same height as the highest peak of the red-brown curve in Figure 38.11. Because of the effect of the square-bracket factor, however, these peaks vary in height as shown.

Equation 37.2 indicates the conditions for interference maxima as $d \sin \theta = m\lambda$, where d is the distance between the two slits. Equation 38.1 specifies that the first diffraction minimum occurs when $a \sin \theta = \lambda$, where a is the slit width. Dividing Equation 37.2 by Equation 38.1 (with $m = 1$) allows us to determine which interference maximum coincides with the first diffraction minimum:

$$\frac{d \sin \theta}{a \sin \theta} = \frac{m\lambda}{\lambda}$$

$$\frac{d}{a} = m \quad (38.7)$$

In Figure 38.11, $d/a = 18 \mu\text{m}/3.0 \mu\text{m} = 6$. Therefore, the sixth interference maximum (if we count the central maximum as $m = 0$) is aligned with the first diffraction minimum and cannot be seen.

Quick Quiz 38.3 Using Figure 38.11 as a starting point, make a sketch of the combined diffraction and interference pattern for 650-nm light waves striking two 3.0- μm slits located 9.0 μm apart.

Quick Quiz 38.4 Consider the central peak in the diffraction envelope in Figure 38.11. Suppose the wavelength of the light is changed to 450 nm. What happens to this central peak? (a) The width of the peak decreases and the number of interference fringes it encloses decreases. (b) The width of the peak decreases and the number of interference fringes it encloses increases. (c) The width of the peak decreases and the number of interference fringes it encloses remains the same. (d) The width of the peak increases and the number of interference fringes it encloses decreases. (e) The width of the peak increases and the number of interference fringes it encloses increases. (f) The width of the peak increases and the number of interference fringes it encloses remains the same.

38.3 Resolution of Single-Slit and Circular Apertures

The ability of optical systems to distinguish between closely spaced objects is limited because of the wave nature of light. To understand this difficulty, consider Figure 38.12, which shows two light sources far from a narrow slit of width a . The sources can be two noncoherent point sources S_1 and S_2 —for example, they could be two distant stars. If no interference occurred between light passing through different parts of the slit, two distinct bright spots (or images) would be observed on the viewing screen. However, because of such interference, each source is imaged as a bright central region flanked by weaker bright and dark fringes—a diffraction pattern. What is observed on the screen is the sum of two diffraction patterns: one from S_1 , and the other from S_2 .

If the two sources are far enough apart to keep their central maxima from overlapping as in Figure 38.12a, their images can be distinguished and are said to be *resolved*. If the sources are close together, however, as in Figure 38.12b, the two central maxima overlap, and the images are not resolved. To determine whether two images are resolved, the following condition is often used:

When the central maximum of one image falls on the first minimum of another image, the images are said to be just resolved. This limiting condition of resolution is known as **Rayleigh's criterion**.

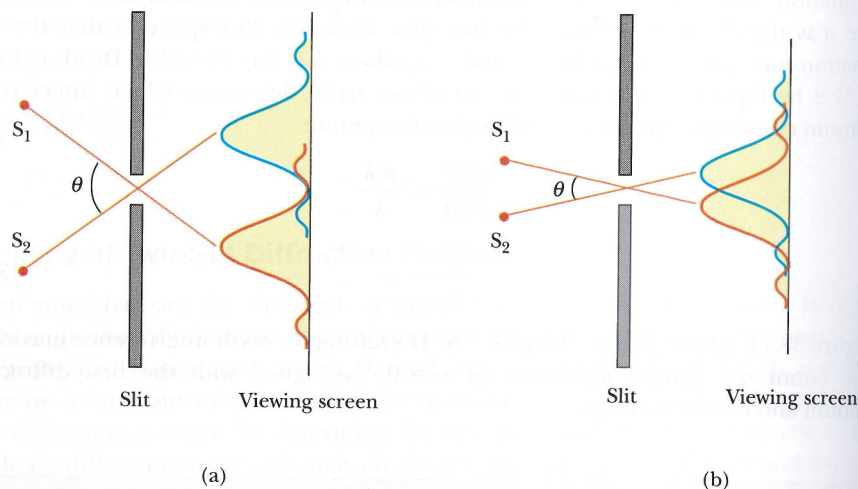


Figure 38.12 Two point sources far from a narrow slit each produce a diffraction pattern. (a) The angle subtended by the sources at the slit is large enough for the diffraction patterns to be distinguishable. (b) The angle subtended by the sources is so small that their diffraction patterns overlap, and the images are not well resolved. (Note that the angles are greatly exaggerated. The drawing is not to scale.)

From Rayleigh's criterion, we can determine the minimum angular separation θ_{\min} subtended by the sources at the slit in Figure 38.12 for which the images are just resolved. Equation 38.1 indicates that the first minimum in a single-slit diffraction pattern occurs at the angle for which

$$\sin \theta = \frac{\lambda}{a}$$

where a is the width of the slit. According to Rayleigh's criterion, this expression gives the smallest angular separation for which the two images are resolved. Because $\lambda \ll a$ in most situations, $\sin \theta$ is small, and we can use the approximation $\sin \theta \approx \theta$. Therefore, the limiting angle of resolution for a slit of width a is

$$\theta_{\min} = \frac{\lambda}{a} \quad (38.8)$$

where θ_{\min} is expressed in radians. Hence, the angle subtended by the two sources at the slit must be greater than λ/a if the images are to be resolved.

Many optical systems use circular apertures rather than slits. The diffraction pattern of a circular aperture, as shown in the lower half of Figure 38.13, consists of a central circular bright disk surrounded by progressively fainter bright and dark rings. Figure 38.13 shows diffraction patterns for three situations in which light from two point sources passes through a circular aperture. When the sources are far apart, their images are well resolved (Fig. 38.13a). When the angular separation of the sources satisfies Rayleigh's criterion, the images are just resolved (Fig. 38.13b). Finally, when the sources are close together, the images are said to be unresolved (Fig. 38.13c).

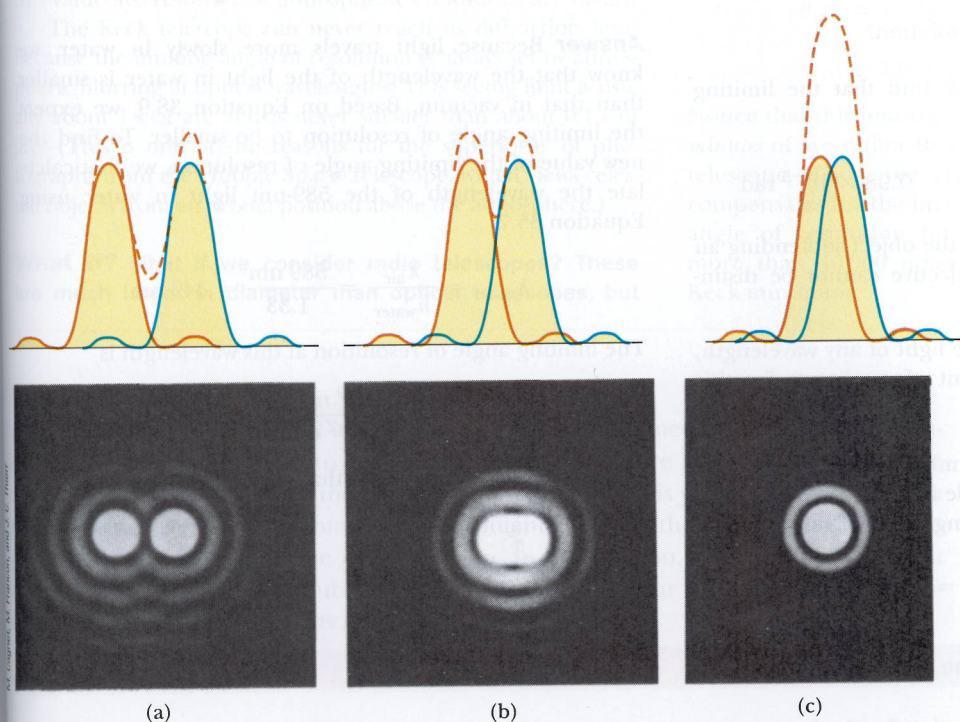


Figure 38.13 Individual diffraction patterns of two point sources (solid curves) and the resultant patterns (dashed curves) for various angular separations of the sources. In each case, the dashed curve is the sum of the two solid curves. (a) The sources are far apart, and the patterns are well resolved. (b) The sources are closer together such that the angular separation just satisfies Rayleigh's criterion, and the patterns are just resolved. (c) The sources are so close together that the patterns are not resolved.

Analysis shows that the limiting angle of resolution of the circular aperture is

Limiting angle of resolution for a circular aperture

$$\theta_{\min} = 1.22 \frac{\lambda}{D} \quad (38.9)$$

where D is the diameter of the aperture. Note that this expression is similar to Equation 38.8 except for the factor 1.22, which arises from a mathematical analysis of diffraction from the circular aperture.

Quick Quiz 38.5 Cat's eyes have pupils that can be modeled as vertical slits. At night, would cats be more successful in resolving (a) headlights on a distant car, or (b) vertically-separated lights on the mast of a distant boat?

Quick Quiz 38.6 Suppose you are observing a binary star with a telescope and are having difficulty resolving the two stars. You decide to use a colored filter to maximize the resolution. (A filter of a given color transmits only that color of light.) What color filter should you choose? (a) blue (b) green (c) yellow (d) red.

Example 38.3 Limiting Resolution of a Microscope

Light of wavelength 589 nm is used to view an object under a microscope. If the aperture of the objective has a diameter of 0.900 cm,

(A) what is the limiting angle of resolution?

Solution Using Equation 38.9, we find that the limiting angle of resolution is

$$\theta_{\min} = 1.22 \left(\frac{589 \times 10^{-9} \text{ m}}{0.900 \times 10^{-2} \text{ m}} \right) = 7.98 \times 10^{-5} \text{ rad}$$

This means that any two points on the object subtending an angle smaller than this at the objective cannot be distinguished in the image.

(B) If it were possible to use visible light of any wavelength, what would be the maximum limit of resolution for this microscope?

Solution To obtain the smallest limiting angle, we have to use the shortest wavelength available in the visible spectrum. Violet light (400 nm) gives a limiting angle of resolution of

$$\theta_{\min} = 1.22 \left(\frac{400 \times 10^{-9} \text{ m}}{0.900 \times 10^{-2} \text{ m}} \right) = 5.42 \times 10^{-5} \text{ rad}$$

What If? Suppose that water ($n = 1.33$) fills the space between the object and the objective. What effect does this have on resolving power when 589-nm light is used?

Answer Because light travels more slowly in water, we know that the wavelength of the light in water is smaller than that in vacuum. Based on Equation 38.9, we expect the limiting angle of resolution to be smaller. To find the new value of the limiting angle of resolution, we first calculate the wavelength of the 589-nm light in water using Equation 35.7:

$$\lambda_{\text{water}} = \frac{\lambda_{\text{air}}}{n_{\text{water}}} = \frac{589 \text{ nm}}{1.33} = 443 \text{ nm}$$

The limiting angle of resolution at this wavelength is

$$\theta_{\min} = 1.22 \left(\frac{443 \times 10^{-9} \text{ m}}{0.900 \times 10^{-2} \text{ m}} \right) = 6.00 \times 10^{-5} \text{ rad}$$

which is indeed smaller than that calculated in part (A).

Example 38.4 Resolution of the Eye

Estimate the limiting angle of resolution for the human eye, assuming its resolution is limited only by diffraction.

Solution Let us choose a wavelength of 500 nm, near the center of the visible spectrum. Although pupil diameter varies from person to person, we estimate a daytime diameter of 2 mm. We use Equation 38.9, taking $\lambda = 500 \text{ nm}$

and $D = 2 \text{ mm}$:

$$\begin{aligned} \theta_{\min} &= 1.22 \frac{\lambda}{D} = 1.22 \left(\frac{5.00 \times 10^{-7} \text{ m}}{2 \times 10^{-3} \text{ m}} \right) \\ &\approx 3 \times 10^{-4} \text{ rad} \approx 1 \text{ min of arc} \end{aligned}$$

38.4

The c
numb
allel g
groov

We can use this result to determine the minimum separation distance d between two point sources that the eye can distinguish if they are a distance L from the observer (Fig. 38.14). Because θ_{\min} is small, we see that

$$\sin \theta_{\min} \approx \theta_{\min} \approx \frac{d}{L}$$

$$d = L\theta_{\min}$$

For example, if the point sources are 25 cm from the eye (the near point), then

$$d = (25 \text{ cm})(3 \times 10^{-4} \text{ rad}) = 8 \times 10^{-3} \text{ cm}$$

This is approximately equal to the thickness of a human hair.

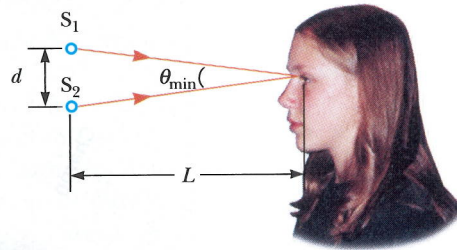


Figure 38.14 (Example 38.4) Two point sources separated by a distance d as observed by the eye.

Example 38.5 Resolution of a Telescope

The Keck telescope at Mauna Kea, Hawaii, has an effective diameter of 10 m. What is its limiting angle of resolution for 600-nm light?

Solution Because $D = 10 \text{ m}$ and $\lambda = 6.00 \times 10^{-7} \text{ m}$, Equation 38.9 gives

$$\theta_{\min} = 1.22 \frac{\lambda}{D} = 1.22 \left(\frac{6.00 \times 10^{-7} \text{ m}}{10 \text{ m}} \right)$$

$$= 7.3 \times 10^{-8} \text{ rad} \approx 0.015 \text{ s of arc}$$

Any two stars that subtend an angle greater than or equal to this value are resolved (if atmospheric conditions are ideal).

The Keck telescope can never reach its diffraction limit because the limiting angle of resolution is always set by atmospheric blurring at optical wavelengths. This seeing limit is usually about 1 s of arc and is never smaller than about 0.1 s of arc. (This is one of the reasons for the superiority of photographs from the Hubble Space Telescope, which views celestial objects from an orbital position above the atmosphere.)

What If? What if we consider radio telescopes? These are much larger in diameter than optical telescopes, but

do they have angular resolutions that are better than optical telescopes? For example, the radio telescope at Arecibo, Puerto Rico, has a diameter of 305 m and is designed to detect radio waves of 0.75-m wavelength. How does its resolution compare to that of the Keck telescope?

Answer The increase in diameter might suggest that radio telescopes would have better resolution, but Equation 38.9 shows that θ_{\min} depends on *both* diameter and wavelength. Calculating the minimum angle of resolution for the radio telescope, we find

$$\theta_{\min} = 1.22 \frac{\lambda}{D} = 1.22 \left(\frac{0.75 \text{ m}}{305 \text{ m}} \right)$$

$$= 3.0 \times 10^{-3} \text{ rad} \approx 10 \text{ min of arc}$$

Notice that this limiting angle of resolution is measured in *minutes* of arc rather than the *seconds* of arc for the optical telescope. Thus, the change in wavelength more than compensates for the increase in diameter, and the limiting angle of resolution for the Arecibo radio telescope is more than 40 000 times larger (that is, *worse*) than the Keck minimum.

As an example of the effects of atmospheric blurring mentioned in Example 38.5, consider telescopic images of Pluto and its moon Charon. Figure 38.15a shows the image taken in 1978 that represents the discovery of Charon. In this photograph taken from an Earth-based telescope, atmospheric turbulence causes the image of Charon to appear only as a bump on the edge of Pluto. In comparison, Figure 38.15b shows a photograph taken with the Hubble Space Telescope. Without the problems of atmospheric turbulence, Pluto and its moon are clearly resolved.

38.4 The Diffraction Grating

The **diffraction grating**, a useful device for analyzing light sources, consists of a large number of equally spaced parallel slits. A *transmission grating* can be made by cutting parallel grooves on a glass plate with a precision ruling machine. The spaces between the grooves are transparent to the light and hence act as separate slits. A *reflection grating* can